Materials and Design 92 (2016) 88–94

Contents lists available at ScienceDirect

Materials and Design

journal homepage: www.elsevier.com/locate/matdes

Hot cracking behavior of carbide-free bainitic weld metals

N. Krishna Murthy, G.D. Janaki Ram *

Department of Metallurgical and Materials Engineering, Indian Institute of Technology Madras, Chennai 600 036, India

ARTICLE INFO

Article history:
Received 29 September 2015
Received in revised form 2 December 2015
Accepted 7 December 2015
Available online 8 December 2015

Keywords:
Carbide-free bainite
Solidification cracking
Varestraint test
Hot ductility test

ABSTRACT

In this work, hot cracking behavior of a carbide-free bainitic weld metal was investigated using Varestraint tests and Gleeble hot ductility tests. The results show that the carbide-free bainitic weld metal is as resistant to hot cracking as many of the standard austenitic stainless steel weld metals. The effects of composition, solidification mode, and impurity content on hot cracking susceptibility of carbide-free bainitic steels are discussed. Some guidelines for optimizing their compositions for superior hot cracking resistance are also presented.

1. Introduction

The present authors have recently demonstrated that carbide-free bainitic (CFB) weld metals can be advantageously utilized in welding of quenched and tempered armor steels for realizing significant gains in weld joint efficiency and ballistic performance without any hydrogen-induced cracking problems [1]. CFB steels typically contain relatively higher carbon, silicon, manganese, chromium, and nickel contents compared to most of the familiar and trusted steel weld metal compositions. Further, they may contain some special alloying elements such as cobalt and aluminum. Because of their rather unusual chemistry, solidification cracking is a potential concern in CFB weld metals [2]. Weld solidification cracking is a complex phenomenon, governed by the metallurgical and thermomechanical processes that occur simultaneously in the mushy zone around the weld pool [3]. According to Kou [4], obstruction of solidification shrinkage and thermal contraction of the semisolid weld metal as well as the surrounding solid base metals induces tensile strain in the semisolid weld metal leading to cracking along the grain boundaries that are not fed with sufficient liquid. Cracking susceptibility is known to be a function of many metallurgical factors such as solidification temperature range, primary solidification phase, amount and distribution of terminal liquid, solute redistribution, dendrite coherence, and solidification grain structure as well as mechanical factors such as thermal contraction, solidification shrinkage, and external restraint [5]. In steels, solidification cracking is generally believed to be a consequence of segregation of impurity and/or alloying elements, leading to the formation of low melting eutectics in the form of continuous inter-granular or inter-dendritic films during the final stages of solidification. These terminal liquid films result in cracking when they fail to accommodate the shrinkage and external tensile stresses acting on the weld.

Another closely related, but different, problem is weld metal heat-affected zone (HAZ) liquation cracking during multi-pass welding. Weld metal HAZ liquation cracking (also referred to as weld metal liquation cracking) is a common problem in many materials. Austenitic stainless steels [6] and nickel-base alloys [7] tend to develop low-melting segregates along the grain boundaries during solidification. In such materials, the weld metal deposited in a pass undergoes incipient melting or liquation of the grain boundaries in the HAZ during the next weld pass. These liquated grains in the HAZ crack because of the tensile stress imposed by the solidifying weld metal. HAZ liquation cracking can occur more easily in weld metals and castings than in standard wrought processed base metals because of their cast, coarse, and segregated microstructure, often with some low-melting eutectics at the grain or dendrite boundaries [5]. CFB weld metals contain a number of alloying elements which can strongly segregate to grain boundaries during solidification. Therefore, weld metal HAZ liquation cracking is a potential concern in CFB weld metals.

At present, no reports are available in open literature on solidification cracking or liquation cracking behavior of carbide-free bainitic weld metals. Detailed understanding in these regards is essential for developing better carbide-free bainitic steel compositions. Therefore, in the current study, hot cracking (fusion zone solidification cracking as well as weld metal HAZ liquation cracking) behavior of a CFB weld metal was investigated using Varestraint tests and Gleeble hot ductility tests to broadly assess its suitability for industrial utilization.

* Corresponding author at: Materials Joining Laboratory, Dept. of Metallurgical and Materials Engineering, Indian Institute of Technology Madras, Chennai 600 036, India.
E-mail address: jram@iitm.ac.in (G.D. Janaki Ram).

http://dx.doi.org/10.1016/j.matdes.2015.12.020
0264-1275/

2. Experimental details

Longitudinal Varestraint tests were conducted on specimens machined from groove welds produced in 6 mm thick plates of an armor-grade quenched and tempered steel (nearly equivalent to AISI 4130). These welds were produced using shielded metal arc welding employing specially developed low-hydrogen basic-coated electrodes using a preheat temperature of 350 °C. After welding, the weld coupons were subjected to post-heating at the same temperature for 6 h to obtain a CFB microstructure in the weld metal. For comparison, tests were also conducted on specimens machined from armor steel welds produced using austenitic stainless steel AWS E307 fillers (without using any preheat). This comparison was considered appropriate because austenitic stainless steel fillers are commonly used at present for welding of armor steels in construction of armored vehicles such as main battle tanks [8]. The chemical compositions of the base and weld metals are listed in Table 1. Fig. 1 shows the Varestraint test specimen. Note that only the weld metal portion of the specimen is remelted during Varestraint testing. Tests were conducted as per AWS B 4.0 on a moving torch Varestraint hot cracking test device (Model LT1100, Materials Applications Inc.) at three strain levels (2, 4, and 6%). At each strain level, five specimens were tested. All the tests were conducted using the same set of welding parameters (current = 90 A, voltage = 12.5 V, travel speed = 2.2 mm/s). After testing, each specimen was examined (after some cleaning and buffing) under a stereomicroscope equipped with a measuring scale at 60× magnification to determine the total crack length (TCL) (sum of the length of all the individual cracks in a given test specimen) and maximum crack length (MCL) (length of the longest crack in a given test specimen). Samples cut from some of these specimens were also examined under an optical microscope after standard metallographic preparation. Elemental mapping studies were also carried out on these samples using a scanning electron microscope (SEM) equipped with Energy Dispersive Spectroscopy (EDS).

Hot ductility tests were conducted on all-weld cylindrical specimens machined from the same welds as those used for Varestraint tests. The test specimen dimensions and the test conditions are given in Table 2. Tests were conducted on a Gleeble 3800 thermo-mechanical simulator (Dyna Systems Inc., USA). Unlike Varestraint testing which attempts to quantify the cracking susceptibility by the degree of cracking, hot ductility testing relates the ductility of the material at elevated temperatures to cracking susceptibility. Detailed information on Gleeble hot ductility testing can be obtained from References [9,10]. It essentially involves the following. Initially, a test is conducted to determine the nil-strength temperature (NST) of the material, which is defined as the temperature on-heating at which the strength of the material drops to essentially zero. In this test, a cylindrical specimen is continuously heated at a certain rate under a constant tensile load of 80 N (just enough to overcome the frictional force of the fixture) until fracture. The temperature at which the specimen fails is noted as the NST. Depending on the test material, the NST can be lower than its nominal solidus temperature. Following this, a series of on-heating tests are conducted to determine the nil-ductility temperature (NDT),

Table 1
Chemical composition of base and weld metals.

Element	Base metal	CFB weld metal	Austenitic weld metal[a]
C	0.3	0.32	0.08
Si	0.7	1.60	0.77
Mn	0.9	1.65	4.92
Ni	0.15	1.15	8.09
Co	–	1.10	0.04
Cr	0.85	1.05	17.5
Mo	0.25	0.27	0.27
S	0.003	0.006	0.004
P	0.010	0.008	0.025

[a] The Ferrite Number (FN) of the austenitic weld metal is 4 (~4 vol.% ferrite).

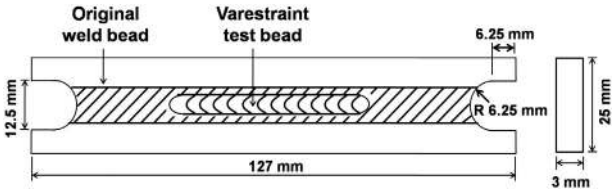

Fig. 1. Varestraint test specimen.

which is defined as the lowest temperature on-heating at which the ductility of the material drops to zero. To begin with, a cylindrical sample is heated at a certain rate to a certain test temperature (typically 100–200 °C lower than the NST temperature) and then it is pulled to failure. The ductility of the specimen is measured in terms of % reduction in area (% RA). Tests are conducted in this manner at successively increasing temperatures until the ductility of the material drops to zero (less than 5% RA). The temperature at which the ductility of the material is zero is noted as the NDT. Following the on-heating tests, a series of on-cooling tests are conducted to determine the ductility-recovery temperature (DRT), which is defined as the highest temperature on-cooling from the NST at which the material exhibits perceptible ductility (more than 5% RA). In these tests, the test specimen is first heated to the NST, cooled to a certain test temperature, and then pulled to failure. The test temperatures are successively lowered and the temperature at which the material exhibits perceptible ductility is noted as the DRT. In the current study, three specimens were tested for determining the NST. On-cooling tests were conducted at the same temperatures as those used for on-heating tests. At each test temperature, both on-heating and on-cooling tests were conducted on at least two specimens. For each specimen, the minimum diameter at the location of fracture was measured using a profile projector and the percentage reduction in area (% RA) was calculated. Longitudinal sections cut from the fractured specimens were prepared for microscopy and microstructures close to the fracture line were examined. Similarly, the fracture surfaces were examined under SEM.

3. Results and discussion

Fig. 2 shows typical solidification cracks in the Varestraint specimens of austenitic and CFB weld metals. In general, cracks appeared radiating from the trailing edge of the weld pool at the instant of straining, as can be seen in Fig. 2a and b. However, in a few CFB weld metal specimens (four out of fifteen), some cracks were found to extend into the weld crater (Fig. 2c). This could be due to some secondary effects and further work is required to understand why crater cracking occurred in CFB welds but not in austenitic welds. In the current study, such crater cracks were not considered in TCL or MCL measurements, as recommended by Lundin et al. [11].

Microstructural examination in the test region of various specimens revealed that the cracks are interdendritic/intergranular, a characteristic feature of solidification cracking (Fig. 3). In CFB weld specimens, EDS elemental mapping studies revealed interdendritic segregation of silicon, manganese, and chromium (Fig. 4). Among the three elements, silicon segregation seemed to be more prominent. Nickel and cobalt, however, did not suffer any noticeable segregation. It is well-known that segregation of alloying elements can promote solidification cracking in steel weld metals. Additionally, in CFB weld metals, it can lead to formation of interdendritic blocky austenite, which is undesirable for the weld metal toughness, as reported by Fang et al. [12]. The results of Varestraint tests are summarized in Fig. 5. In both CFB and austenitic weld metals, the TCL and MCL increased with the applied strain. The cracking data obtained for the austenitic weld metal in the current study is consistent with the findings of earlier investigations for similar compositions [13–15]. Importantly, at any given strain level, the TCL and MCL values for the CFB weld metal are only slightly higher compared to

Table 2
Gleeble hot ductility test conditions.

Parameter	NST	On-heating	On-cooling
Specimen	Cylindrical, 6 mm diameter and 90 mm length	Cylindrical, 6 mm diameter and 106.5 mm length, M6 × 1.00–6 g thread on both ends (thread length: 15.25 mm)	
Jaws and grips	Low-force jaws and half-contact copper grips	Standard jaws and full-contact copper grips	
Sample free span	15 mm		
Thermocouple	Type B (Pt-30%Rh/Pt-6%Rh)		
Atmosphere	Vacuum (2×10^{-4} Torr)		
Heating rate	25 °C/s up to 1150 °C and 2 °C/s thereafter	100 °C/s	
Test temperature	–	1250 °C, 1275 °C, 1300 °C, 1325 °C[a]	
Cooling rate	–	–	25 °C/s (from NST to test temperature)
Holding time	–	0.5 s	
Stroke rate	–	25 mm/s	
Others	Constant tensile load: 80 N	–	

[a] On-cooling test specimens were first heated to the NST, held for 0.5 s, and then cooled to the test temperature.

the austenitic weld metal, which is considered highly crack resistant and is in successful industrial use for welding of armor steels.

Solidification cracking in steels is known to be strong function of the weld metal chemistry, which governs the mode of solidification. In general, compositions which solidify in austenite mode are more susceptible to solidification cracking than those that solidify in ferrite mode [16]. This is because sulfur and phosphorus, the common impurity elements found in steels, have significantly lower solubility in austenite than in ferrite. Consequently, during solidification in austenite mode these impurity elements strongly segregate to the liquid, extending the freezing range and eventually resulting in some undesirable low-melting eutectics. Many of the standard structural steel weld metals solidify in ferrite mode and are therefore more tolerant to the detrimental effects of sulfur and phosphorus. Conversely, in certain low alloy steels, such as Fe–C–Ni alloys with low levels of sulfur and phosphorus, solidification in austenite mode is known to be beneficial for solidification cracking resistance [17]. The main reason is that both carbon and nickel segregate less when solidification occurs in austenite mode than in ferrite mode (both elements have a higher partition efficient in austenite). Further, in binary Fe–C alloys with carbon in the range of 0.09 to 0.11 wt.% (which solidify in ferrite mode), it has been shown that solidification cracking is aided by enhanced shrinkage stress imposed by $\delta \rightarrow \gamma$ transformation taking place within the brittleness temperature range. Thus, while it is generally believed that solidification in ferrite mode is beneficial for solidification cracking resistance of steels, there are some cases where it does not hold good.

The effect of solidification mode on cracking susceptibility is also well-established in austenitic stainless steels [18,19]. Depending on the ratio of chromium and nickel equivalents, austenitic stainless steel weld metals can solidify in austenite, primary austenite, primary ferrite, or ferrite modes. Alloys that solidify in austenite mode are most susceptible and those that solidify in primary ferrite mode are least susceptible to solidification cracking. The austenitic weld metal under consideration in this study solidified in primary ferrite mode, as revealed by the skeletal morphology of δ-ferrite in its room temperature microstructure [1]. Feritscope measurements indicated that the δ-ferrite content in the present austenitic weld metal is ~4 vol.%.

Calculations using Thermo-Calc software (TCFE7 database) suggest that the CFB weld metal under consideration in the current study solidifies in austenite mode (liquidus ~1472 °C, solidus ~1400 °C, under

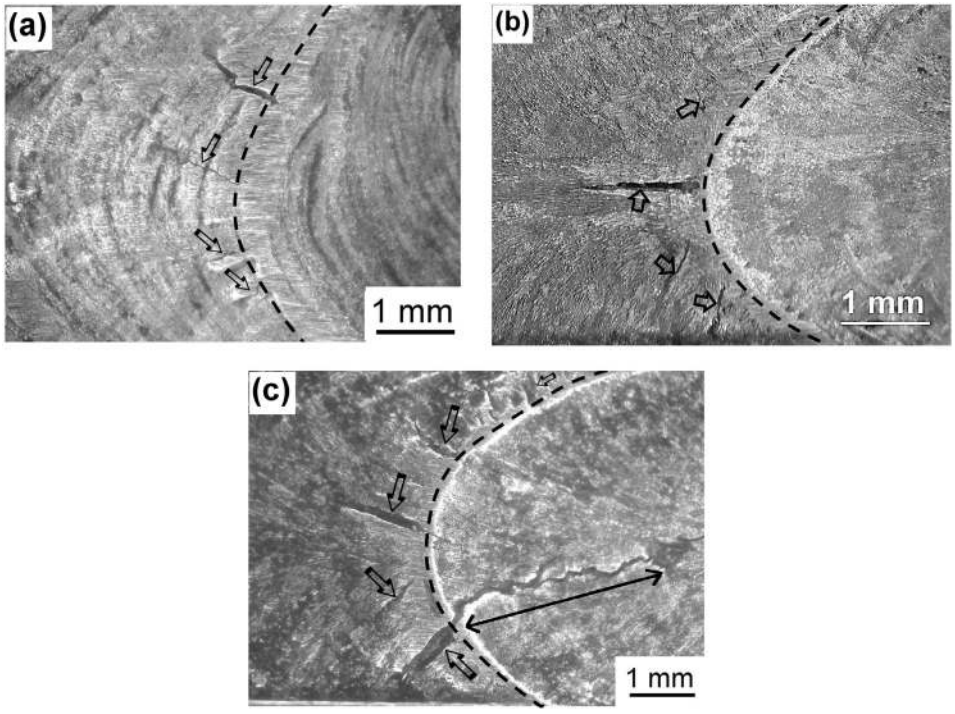

Fig. 2. Macrographs of austenitic (a) and CFB (b and c) weld specimens (top surfaces) after Varestraint testing at 6% strain. Dashed lines mark the trailing edge of the weld pool at the instant of straining (identified by observing the ripple lines on the specimen surface). Note the crater crack in (c). The length of the crack inside the weld crater (marked by double-headed arrow) was not considered in quantitative analysis of cracking susceptibility.

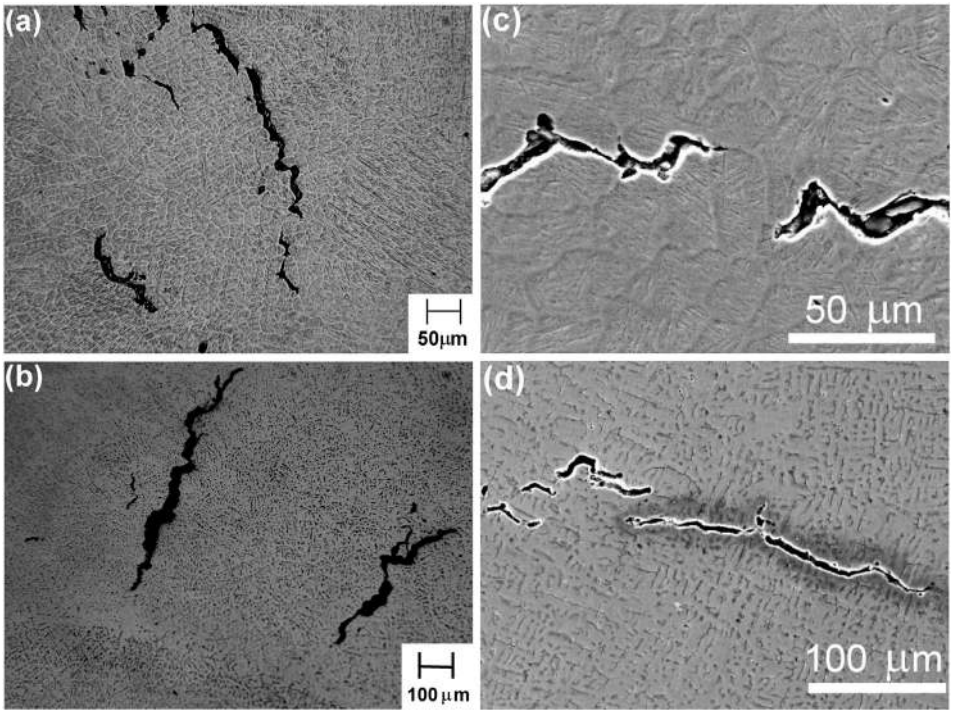

Fig. 3. Optical and SEM micrographs of CFB (a and c) and austenitic (b and d) weld specimens after Varestraint testing at 6% strain.

equilibrium conditions). This is likely to be case for many of the known bulk CFB steel compositions [2]. Thus, in CFB weld metals, control of impurity elements assumes greater significance. Their impurity tolerance can be enhanced by suitably modifying their compositions for obtaining ferrite mode of solidification. Reduction in austenite stabilizers such as carbon, manganese, and nickel and additions of strong ferrite stabilizers such as aluminum should be considered for this purpose. Apart from promoting austenite mode of solidification, carbon can significantly widen the solidification range [16]. Keeping the carbon content in the range of 0.2 to 0.3 wt.% is thus the single most important consideration in realizing CFB weld metals with satisfactory solidification cracking resistance. It should be noted that it may not desirable to reduce the carbon content further in CFB weld metals because of three reasons. First, as the carbon content is decreased, the martensite start (M_S) temperature of the weld metal increases. Consequently, one must carry out welding using a higher preheat temperature (for obtaining a

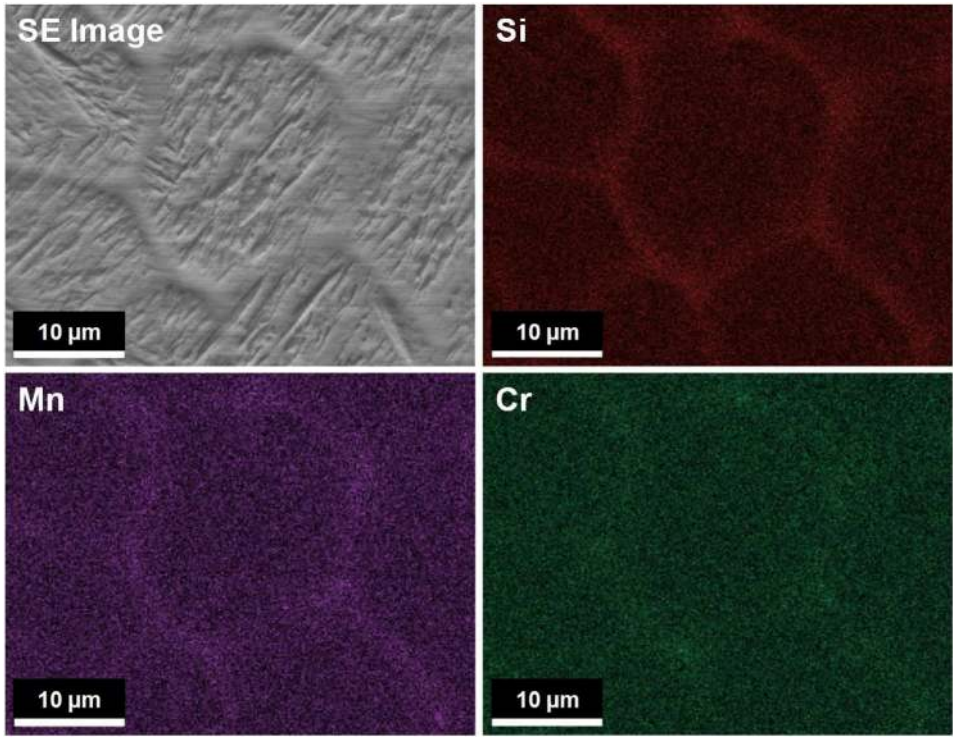

Fig. 4. EDS elemental maps of CFB weld metal. Note interdendritic segregation of silicon, manganese, and chromium.

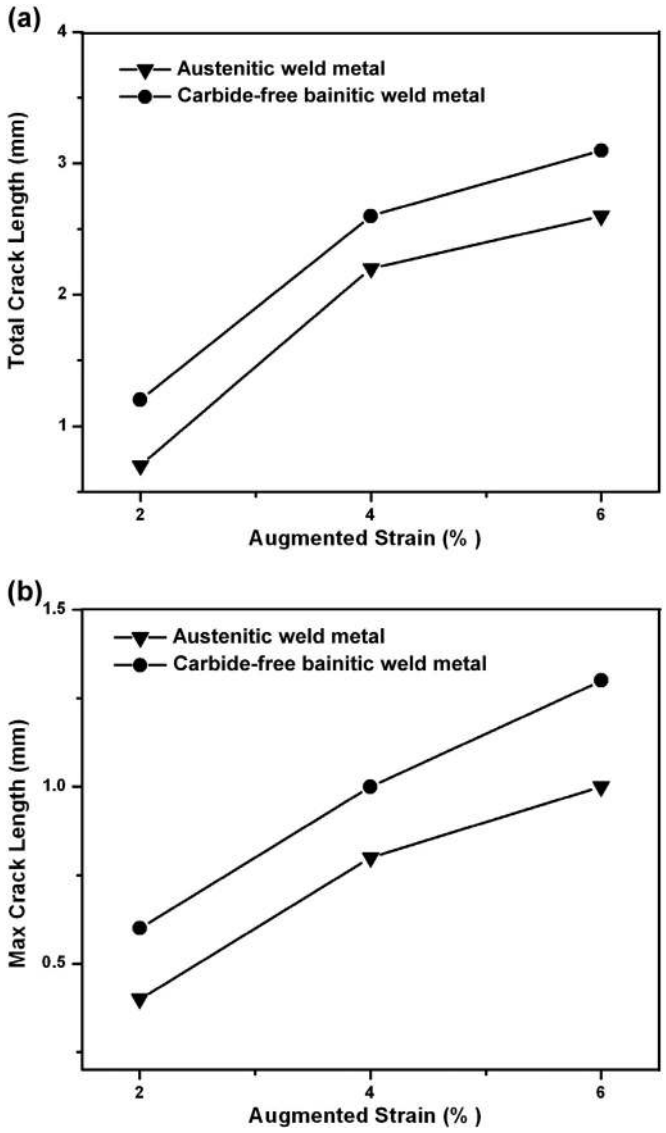

Fig. 5. Varestraint test results: (a) TCL vs. strain, (b) MCL vs. strain.

carbide-free bainitic microstructure, the preheat temperature must be above the M_S temperature of the weld metal). As the carbon content is reduced further and further, at some point, the preheat temperature would become impractically high (such high preheat temperatures can affect the base metal microstructure and properties as well). Secondly, as the carbon content is reduced, the temperature at which bainitic transformation is realized increases. This can affect the scale of the microstructure (thickness of ferrite plates) as well as the volume fraction of bainite that can be produced [20,21]. Further, as recently shown by Long et al. [22], an increase in the transformation temperature can decrease the high-angle misorientation fraction in packets of bainite ferrite plates and, hence, can affect the toughness of carbide-free bainitic steels. More importantly, the carbon content can directly influence the strength of carbide-free bainite [23]. Thus, at very low levels of carbon, the carbide-free bainitic weld metal may not satisfy the strength requirements. For these reasons, the authors believe that, in carbide-free bainitic weld metals, a carbon content in the range of 0.2 to 0.3 wt.% offers the best trade-off between solidification cracking resistance and transformation behavior and/or weld mechanical properties. A carbon content within this range also benefits the formability of carbide-free bainitic steels, a key requirement in automotive industry [24].

With regard to other alloying elements, while manganese is certainly needed in CFB weld metals in sufficient amount for fixing sulfur, its excessive use should be avoided as it is known to promote solidification cracking [16]. Very often, in bulk CFB steels, manganese is primarily used for hardenability. In CFB weld metals, however, this is not an important requirement (because of the inherently high cooling rates in welding). Manganese reduction also serves to accelerate bainite formation at low temperatures [25]. Similarly, one can think of reducing nickel to the bare minimum or even totally eliminating it, although the latter needs to be carefully considered as it might impair the weld metal toughness. Chromium and cobalt do not seem to have any strong negative effects on hot cracking resistance; hence they can be considered for use in CFB weld metals as appropriate based on other considerations. More importantly, it is known that silicon at levels above 0.65 wt.% can promote hot cracking in steels [16,26]. Therefore, partial replacement of silicon with aluminum, which is also a potent graphitizer, can be very helpful. As recently shown by Huang [25], aluminum and silicon are equally effective in suppressing cementite formation. Aluminum additions can be additionally beneficial for accelerating the bainitic transformation kinetics [27]. It should be noted that optimization of CFB weld metal compositions cannot be done entirely on the basis of hot cracking resistance. Many other factors such as temperature and time of bainitic transformation, formation of undesirable blocky austenite, and weld metal strength and toughness need to be considered along with hot cracking resistance.

The results of Gleeble hot ductility tests are shown in Fig. 6. The NST, NDT, and DRT temperatures for the CFB weld metal were determined as 1350 °C, 1325 °C, and 1300 °C, respectively. The on-heating ductility was nearly 100% at 1250 °C, but decreased sharply as the test temperature was increased and approached zero at 1325 °C. On cooling from NST, the CFB weld metal did not recover ductility until it had been cooled to 1300 °C; at temperatures further below, the on-cooling ductilities were as good as on-heating ductilities. It should be noted that hot ductility tests in this study were conducted on weld metal specimens. Thus, the starting microstructure of all the test specimens was as-cast, with some built-in compositional inhomogeneities that had occurred during original weld metal solidification (as seen in Fig. 4). This has a bearing, in particular, on the results of on-heating tests. The NDT and NST temperatures would have been considerably higher had the starting material been well-homogenized and wrought. This also explains why the on-cooling curve closely followed the on-heating curve. Nevertheless, some useful inferences can be made from these tests.

During welding, the material loses all its ductility when the temperature reaches the NDT on heating. It does not regain any ductility until the DRT is reached on cooling. Thus, during welding, the material passes

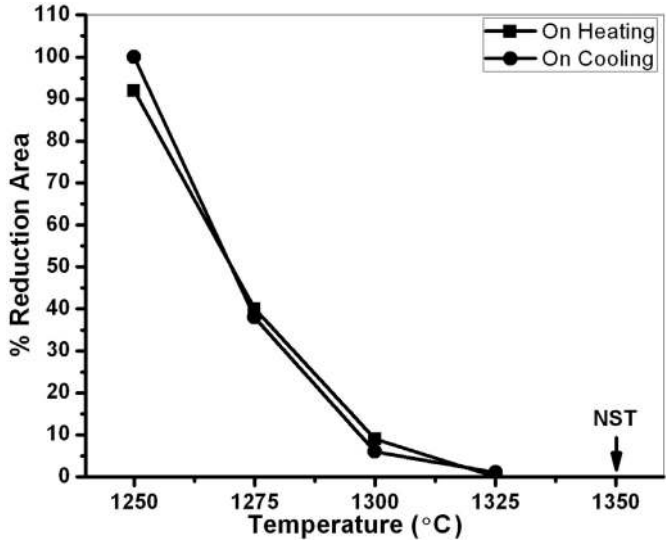

Fig. 6. Hot ductility test results.

through two different temperature ranges over which the ductility of the material is essentially zero [10]: (i) on-heating nil-ductility temperature range (the temperature range from the NDT to the liquidus temperature), and (ii) on-cooling nil-ductility temperature range (the temperature range from the liquidus temperature to the DRT). Unlike the on-heating nil-ductility temperature range, the on-cooling nil-ductility temperature range is not a fixed for a given material as the DRT is a function of the peak temperature that the material is subjected to during welding. With increasing peak temperature above the NDT, the DRT decreases, widening the on-cooling nil-ductility temperature range. Thus, the DRT would be the lowest for a peak temperature equal to the liquidus temperature of the material. While it is most appropriate to consider this DRT in any analysis on solidification cracking, conducting on-cooling tests using peak temperatures above the NST of the material is extremely difficult in a standard Gleeble hot ductility test set-up [10]. Therefore, it is customary to determine the DRT using a peak temperature equal to the NST of the material, as is done in the current study.

Essentially, for a solidification crack to develop, there must be a region in the solidifying weld metal with a crack-susceptible microstructure and it must be subjected to high enough tensile strain or stress. Normally, until the weld begins to cool and solidification progresses to an advanced stage, sufficient tensile strain or stress does not develop. Although many different solidification cracking theories have been proposed to date, all of them are in general agreement that cracking occurs in a discrete temperature range, called the brittleness temperature range (BTR) [10]. This is generally considered as the temperature range from the NST to the DRT. It represents a temperature range where liquid is confined within the solidification structure. Within the BTR, the ductility of the material is essentially zero and the material is thus susceptible to cracking. Below the BTR, the terminal liquid is almost completely solidified and the material recovers its ductility. In essence, the wider the BTR, the more susceptible the material is for solidification cracking. This temperature range is quite narrow for the present CFB weld metal (about 50 K). Many standard austenitic stainless steel weld metals that are known to be reasonably crack resistant exhibit similar BTRs [10,15]. However, for reasons explained above, the BTR in the current case is better considered as the temperature range from the nominal solidus of the CFB weld metal (calculated using Thermo-Calc as 1400 °C) to the DRT (1300 °C). Even this temperature range is not very wide (about 100 °C). Thus, the solidification cracking resistance of the present CFB weld metal seems to be quite good.

The hot ductility tests conducted in this study can throw some light on the weld metal HAZ liquation cracking, which is, of course, an issue only in multi-pass welds or in repair welds. The on-heating nil-ductility temperature range (from the NDT to the nominal solidus temperature) is about 75 °C. This temperature range determines the extent of weld metal HAZ which suffers liquation during welding. Another temperature range to be considered here is the BTR (from the NST to the DRT). This represents the temperature range over which cracking can actually take place. In this case, it is not unreasonable to use the NST as the basis as it was determined for the weld metal itself. Both these temperature ranges are reasonably narrow and, hence, the present CFB weld metal can be expected to be quite resistant to weld metal HAZ liquation cracking.

Fig. 7 shows the optical micrographs of the various hot ductility test specimens (close to fracture line). In general, all the specimens that fractured without much plastic deformation showed extensive intergranular secondary cracking (for example, Fig. 7a, c, d, and e). On the other hand, specimens that failed after significant plastic deformation showed several deformation voids elongated in the loading direction (for example, Fig. 7b and f).

Fig. 8 shows the SEM fractographs of the various hot ductility test specimens. All the specimens revealed intergranular fracture features. Intergranular fracture is common at high temperatures and can occur even in the absence of grain boundary liquid films — for example, the specimens tested on-heating as well as on-cooling at 1275 °C show intergranular fractures (Fig. 8b and f). In the NST test specimens, the grains appeared distinctly coarse and rounded (Fig. 8a). As the material is heated to the NST, it would undergo considerable grain coarsening and incipient melting of the grain boundaries. In on-heating specimens, the grain size was observed to increase with the test temperature (compare Fig. 8b, c, and d). Understandably, grain coarsening becomes more and more significant as the test temperature increases. Further, during hot ductility testing, specimens can undergo dynamic recrystallization if they fail after significant plastic formation [28]. These factors can explain why the fracture surfaces of the specimens tested on-heating at 1250 °C and 1275 °C showed relatively finer grains compared those that were tested at 1300 °C and 1325 °C. The specimens tested on-cooling at 1325 °C and 1300 °C showed more or less the same grain size

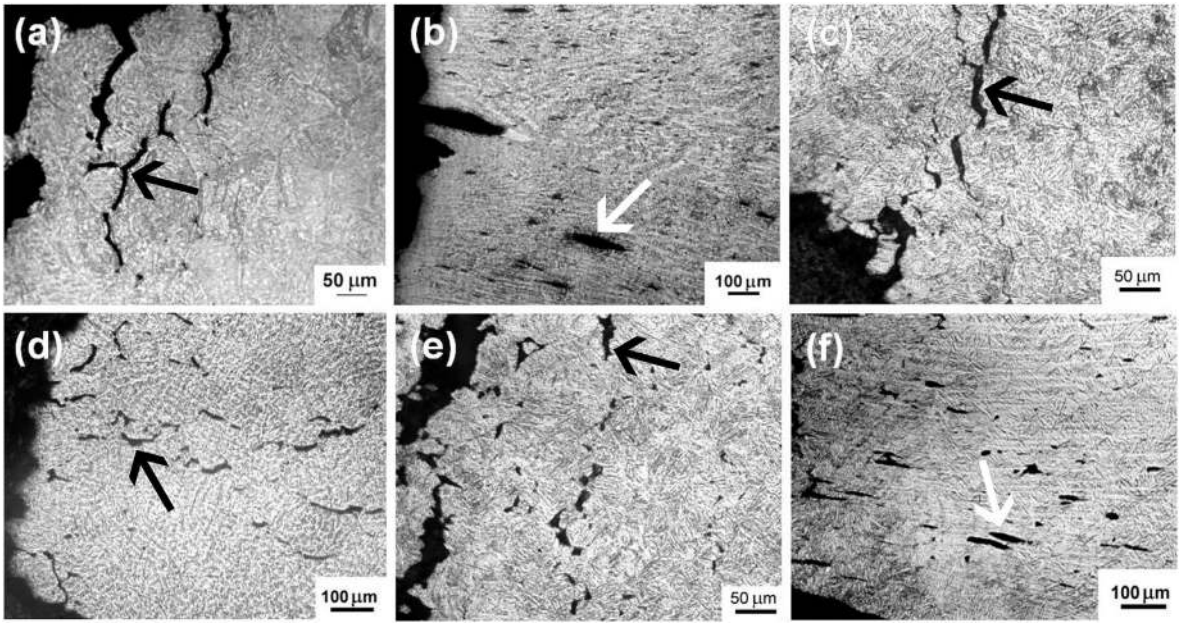

Fig. 7. Microstructures of hot ductility test specimens (close to fracture line): (a) NST, (b) on-heating, 1275 °C, (c) on-heating, 1300 °C, (d) on-heating, 1325 °C, (e) on-cooling, 1300 °C, (f) on-cooling, 1275 °C. Black arrows in (a), (c), (d) and (e) show some secondary cracks. White arrows in (b) and (f) show some elongated voids due to extensive plastic deformation.

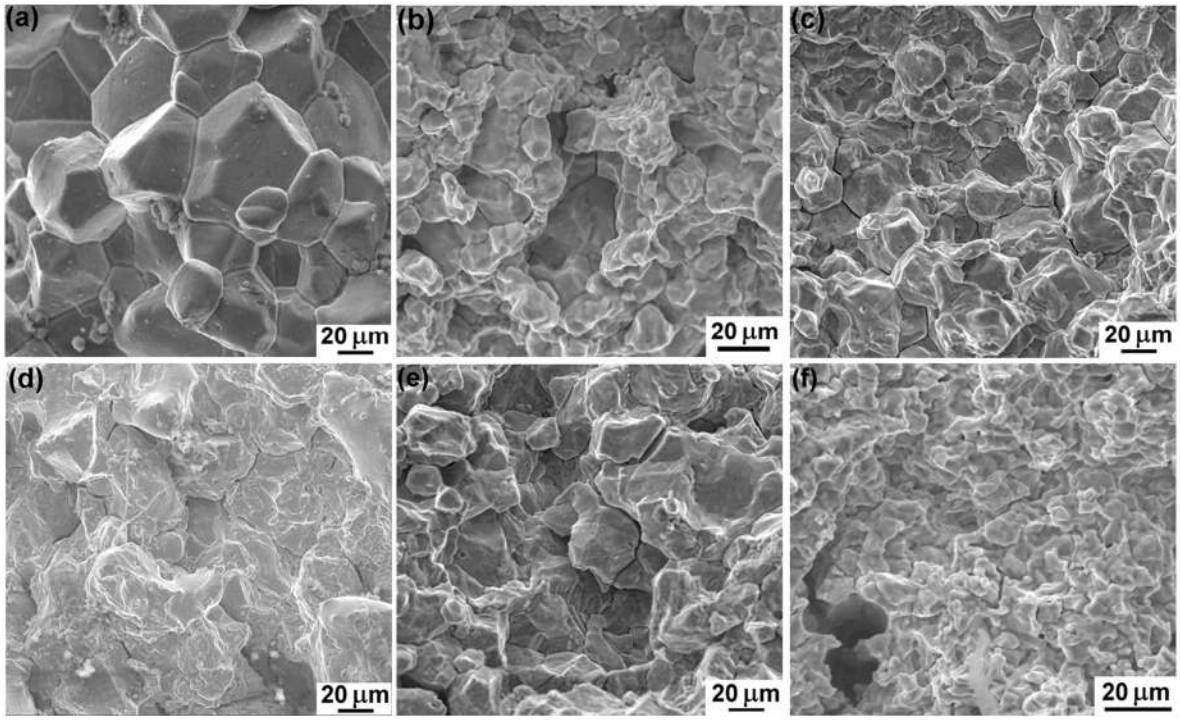

Fig. 8. Fractographs of hot ductility test specimens: (a) NST, (b) on-heating, 1275 °C, (c) on-heating, 1300 °C, (d) on-heating, 1325 °C, (e) on-cooling, 1300 °C, (f) on-cooling, 1275 °C.

as the NST test specimens (compare Fig. 8a and e). This is understandable as these specimens were first heated to the NST temperature and they fractured without any significant plastic deformation. However, the specimens tested on-cooling at 1275 °C and 1250 °C showed finer grains although these were also first heated to the NST temperature (Fig. 8f). As noted earlier, these specimens fractured after significant plastic deformation and, in the process, developed a finer grain size due to dynamic recrystallization.

4. Summary

The current study shows that carbide-free bainitic weld metals (with around 0.3 wt.% carbon) are not seriously susceptible to fusion zone solidification cracking or weld metal HAZ liquation cracking. They are as resistant to hot cracking as many of the standard austenitic stainless steel weld metals. Hence, they are suitable for use in heavy structural fabrication work such as in construction of main battle tanks for welding of quenched and tempered armor steels. Compared to standard low alloy steel weld metals, carbide-free bainitic weld metals may call for a tighter control over harmful impurities such as sulfur and phosphorus because of their tendency to solidify in austenite mode. Similarly, when using carbide-free bainitic weld metals, it may be necessary to closely control the fusion zone solidification structure and weld bead shape and geometry to minimize hot cracking problems. The authors believe that it may be possible to develop carbide-free bainitic weld metals with superior hot cracking resistance by reducing the carbon content, partially replacing silicon with aluminum, and adjusting other alloying elements for obtaining ferrite mode of solidification.

Acknowledgments

The authors are grateful to Armament Research Board, Defence Research and Development Organisation, Ministry of Defence, Govt. of India (ARMREB/MAA/2010/119), for funding this work. The authors gratefully acknowledge the financial support through FIST program from Department of Science and Technology, Govt. of India (SR/FST/ETII-049/2011), for establishing a Gleeble thermo-mechanical simulation facility at IIT Madras. The authors express their sincere thanks to Controllerate of Quality Assurance (Heavy Vehicles) and Heavy Vehicle Factory, Avadi, Chennai, India, for facilitating welding experiments.

References

[1] N. Krishna Murthy, G.D. Janaki Ram, B.S. Murty, G.M. Reddy, T.J.P. Rao, Carbide-free bainitic weld metal: a new concept in welding of armor steels, Metall. Mater. Trans. B Process Metall. Mater. Process. Sci. 45 (2014) 2327–2337.
[2] F.G. Caballero, M.J. Santofimia, C. Captivila, C. Garcia-Mateo, C. Garcia de Andres, Mater. Des. (2009) 2077–2083.
[3] C.E. Cross, in: T. Bollinghaus, H. Herold (Eds.), Hot Cracking Phenomena in Welds, Springer 2005, pp. 3–18.
[4] S. Kou, Acta Mater. 88 (2015) 366–374.
[5] S. Kou, JOM (2003) 37–42.
[6] C.D. Lundin, C.P.D. Chou, Weld. J. 64 (1985) 113s–118s.
[7] W.A. Baeslack, W.P. Lata, S.L. West, Weld. J. (1988) 77s–87s.
[8] S.J. Alkemade, The Weld Cracking Susceptibility of High Hardness Armour Steel, Report # DSTO-TR-0320, Defence Science and Technology Organisation, Australia, 1996.
[9] S.T. Mandziej, in: T. Bollinghaus, H. Herold (Eds.), Hot Cracking Phenomena in Welds, Springer 2005, pp. 347–376.
[10] W. Lin, J.C. Lippold, W.A. Baeslack III, Weld. J. (1993) 135s–153s.
[11] C.D. Lundin, A.C. Lingenfelter, G.E. Grotke, G.G. Lessmann, S.J. Matthews, The Varestraint Test, WRC Bulletin # 280, Welding Research Council, New York, USA, 1982 1–19.
[12] K. Fang, J.G. Yang, X.S. Liu, K.J. Song, H.Y. Fang, H.K.D.H. Bhadeshia, Mater. Des. 50 (2013) 38–43.
[13] C.D. Lundin, C.H. Lee, R. Menon, Weld. J. (1988) 119s–130s.
[14] C.D. Lundin, C.Y.P. Qiao, T.P.S. Gill, G.M. Goodwin, Weld. J. (1993) 189s–200s.
[15] V. Shankar, T.P.S. Gill, S.L. Mannan, S. Sundaresan, Sci. Technol. Weld. Join. (2000) 91–97.
[16] N. Bailey, Weldability of Ferritic Steels, Abington Publishing, Cambridge, England, 1994 54–74.
[17] V. Shankar, J.H. Devletian, Sci. Technol. Weld. Join. (2005) 236–243.
[18] V. Shankar, T.P.S. Gill, S.L. Mannan, S. Sundaresan, Sadhana (2003) 359–382.
[19] J.C. Lippold, D.J. Kotecki, Welding Metallurgy and Weldability of Stainless Steels, Wiley-Interscience, New Jersey, USA, 2005 164–173.
[20] S. Khare, K. Lee, H.K.D.H. Bhadeshia, Metall. Trans. A 41 (2010) 922–928.
[21] D. Mandal, M. Ghosh, J. Pal, S.G. Chowdhury, G. Das, S.K. Das, S. Ghosh, Mater. Des. 54 (2014) 831–837.
[22] X.Y. Long, J. Kang, B. Lv, F.C. Zhang, Mater. Des. 64 (2014) 237–245.
[23] M. Soliman, H. Palkowski, Prod. Eng. 81 (2014) 1306–1311.
[24] F.G. Caballero, S. Allain, J. Cornide, J.D. Puerta Velásquez, C. Garcia-Mateo, M.K. Miller, Mater. Des. 49 (2013) 667–680.
[25] H. Huang, M.Y. Sherif, P.E.J. Rivera-Díaz-del-Castillo, Acta Mater. 61 (2013) 1639–1647.
[26] J. Yu, M. Rombouts, G. Maes, Mater. Des. 45 (2013) 228–235.
[27] L. Qian, Q. Zhou, F. Zhang, J. Meng, M. Zhang, Y. Tian, Mater. Des. (2012) 264–268.
[28] B. Weiss, G.E. Grotke, R. Stickler, Weld. J. (1970) 471s–487s.